

Water Diffusion Compartmentation and Anisotropy at High b Values in the Human Brain

Chris A. Clark* and Denis Le Bihan

Biexponential diffusion decay is demonstrated in the human brain in vivo using b factors up to 4000 sec mm⁻². Fitting of the signal decay data yields values for the slow and fast diffusion components and volume fractions in agreement with previous studies in rat and human brain. In addition, differences in the fitted parameters are demonstrated in the white and gray matter and diffusion anisotropy is demonstrated in both the slow and fast diffusing components. Apparent anisotropy in the component fractions is discussed in terms of directionally dependent exchange rates between the compartments. The lack of a relationship between the estimated contribution to the signal of the fast and slow components and echo time appears to rule out T_2 differences in the observed water compartments. Values obtained for the fast diffusion coefficient, including differences between white and gray matter and the degree of anisotropy are compatible with the predictions of extracellular diffusion of water based on tortuosity models and the diffusion of tetramethylammonium ions in rat brain. Magn Reson Med 44: 852–859, 2000. © 2000 Wiley-Liss, Inc.

Key words: diffusion; compartmentation; anisotropy; brain; MRI

Water diffusion in the brain is two to 10 times smaller than free water diffusion due to the presence of the tissue microstructure, which impedes molecular displacements. Diffusion is exquisitely sensitive to cellular geometric features, such as cell size (reduced diffusion in cytotoxic edema) and orientation (diffusion anisotropy in white matter), leading to important clinical applications. Diffusion imaging has been used to quantitatively characterize normal brain tissue (1), stroke infarcts (2), multiple sclerosis (MS) lesions (3), normal-appearing white matter (3), tumors (4), hippocampal sclerosis in epilepsy (5), Creutzfeldt-Jakob disease (6), schizophrenia (7), brain injury (8), and other pathologies.

Yet the exact mechanisms underlying the link between diffusion and tissue microstructure remain largely unknown (9). High viscosity and restriction effects have been proposed for water diffusion in the intracellular space, and tortuosity effects described for water diffusion in the extracellular space. It is thus important to evaluate the respective contributions of the intra- and extracellular compartments in order to provide a better understanding of the overall water diffusion characteristics of the tissue. So far, most studies performed with conventional MRI hardware and limited gradient power report diffusion measurements in terms of a single, global parameter, the apparent diffusion coefficient (ADC), whereby the diffusion signal decay is assumed to be monoexponential.

The diffusion model may be refined, however, by including anisotropy and tissue orientation information (by measuring changes in the ADC according to gradient orientation) (10–12) and restricted diffusion effects by changing the diffusion time (13,14). Furthermore, MR diffusion imaging experiments using high b values (>1000 sec mm⁻²) have shown that the diffusion signal decay is no longer monoexponential, but is more accurately described in terms of a biexponential function of the form

$$\frac{S(b)}{S(0)} = f_{\text{slow}} \exp(-b \cdot \text{ADC}_{\text{slow}}) + f_{\text{fast}} \exp(-b \cdot \text{ADC}_{\text{fast}}) \quad [1]$$

where $S(b)$ is the signal in the presence of diffusion sensitization, $S(0)$ is the signal in the absence of diffusion sensitization, ADC_{slow} and ADC_{fast} represent the fast and slow diffusing ADCs, and f_{slow} and f_{fast} represent the contribution to the signal of the slow and fast diffusing water compartments. This model assumes that exchange is slow between the two compartments during the diffusion measurement time t_D .

Studies performed by Niendorf et al. (15) in the rat brain in vivo (with b factors up to 10000 sec mm⁻²) using this model yielded $\text{ADC}_{\text{fast}} = (8.24 \pm 0.30) \times 10^{-4}$ mm² sec⁻¹ and $\text{ADC}_{\text{slow}} = (1.68 \pm 0.10) \times 10^{-4}$ mm² sec⁻¹ with $f_{\text{fast}} = 0.80 \pm 0.02$ and $f_{\text{slow}} = 0.17 \pm 0.02$. The volume fractions of the two water compartments obtained by Niendorf et al. did not, however, agree with those expected for the intra- and extracellular water fractions; $F_{\text{intra}} = 0.80$ and $F_{\text{extra}} = 0.20$ (16) given that extracellular water is considered to be more rapidly diffusing than intracellular water. This would appear to challenge the validity of the assumptions embodied in Eq [1]. Niendorf et al. ruled out different T_2 contributions from each compartment, which may have explained this discrepancy, by demonstrating invariance of the estimated parameters at two different echo times of 50 and 90 msec.

Similar results were obtained by Mulkern et al. (17) in the human brain in vivo using b factors up to 6000 sec mm⁻². Using a volume localized technique in eight subjects, values similar to those of Niendorf et al. (15) were obtained. Based on the discrepancy between the measured volume fractions and those in the literature, Mulkern et al. (17) also concluded that Eq. [1] appeared to be inadequate to describe the diffusion compartmentation in human brain.

An important issue that these previous in vivo studies have not addressed, however, is that of anisotropy. Diffusion anisotropy in white matter is a sensitive marker of structural integrity and a number of studies, notably those based on the diffusion tensor, have revealed structural modifications in MS (3) and schizophrenic brains (7). Diffusion anisotropy also forms the basis of new fiber-tracking

Department of Medical Research, Service Hospitalier Frederic Joliot, Orsay, France.

Grant sponsor: EEC BioMed; Grant number: BMH4-CT96-0870.

*Correspondence to: Chris A. Clark, Ph.D., Lucas MRSI Center, 1201 Welch Road, Stanford, CA 94305. E-mail: chris@s-word.stanford.edu

Received 4 October 1999; revised 10 July 2000; accepted 19 July 2000.

© 2000 Wiley-Liss, Inc.

methods based on the directional similarity of the principal eigenvectors obtained from the diagonalized diffusion tensors in adjacent voxels (18–21). The mechanisms responsible for diffusion anisotropy in white matter are thought to involve a greater restriction or hindrance of water molecule mobility across fiber tracts (axon cylinders and myelin sheaths) than along them. Clearly, an investigation into the directional properties of compartmentalized water diffusion may further elucidate the nature of white matter diffusion anisotropy in human brain. Furthermore, an investigation into the transverse relaxation properties of the two compartments has yet to be performed *in vivo*.

The availability of new more powerful gradient hardware on clinical MRI systems offers the opportunity to study human brain water diffusion at much larger b factors ($>1000 \text{ sec mm}^{-2}$) than have been used previously. Gradient coils, capable of producing magnetic field gradients of up to 40 mT m^{-1} on a clinical MRI system operating at 1.5 T, were used to demonstrate biexponential diffusion attenuation in the human brain *in vivo*. These experiments were designed to 1) investigate possible changes in the diffusion coefficients and the fractional contribution to the signal of the two resolved water components at two different diffusion times, 2) identify possible differences in diffusion compartmentation in white and gray matter, 3) elucidate the role of transverse relaxation in determining the estimated volume fractions of the two components, and 4) examine anisotropy of the fast and slow diffusing components in white matter.

METHOD

The study, approved by the Institutional Ethics Committee, was performed on five healthy volunteers, each of whom gave informed consent. Diffusion imaging was performed on a whole body 1.5T MRI system (Signa, General Electric Medical Systems, Milwaukee, MN) equipped with an actively shielded whole-body magnetic field gradient set allowing up to 40 mT m^{-1} .

An echo planar imaging sequence, sensitized to diffusion by application of additional gradient pulses either side of the refocusing RF pulse, was used to provide images with diffusion weighting (on all three gradient axes simultaneously, so as to maintain TE as short as possible) increasing the value of the b factor, linearly from 0 to 3800 sec mm^{-2} . To validate the performance of the sequence, diffusion-weighted images were obtained at a single slice location in a phantom containing isopropanol at 22°C and the diffusion coefficient was calculated assuming a monoexponential decay.

For the initial human brain study, the diffusion sequence was preceded with an inversion pulse so as to suppress the contribution of CSF to the signal (which may potentially result in a biexponential signal decay). Forty-five diffusion-weighted images were collected in addition to five initial images acquired in the absence of diffusion sensitization to ensure that the NMR signal achieved a steady state. These images were subsequently discarded from the signal decay analysis. Each acquisition included 10 axial planes, providing a total of 500 images. For each subject, two experiments were performed at diffusion

times corresponding to $t_D = 24.7 \text{ msec}$ and $t_D = 57.7 \text{ msec}$. Additional imaging parameters used for both sequences were: slice thickness = 5 mm, slice gap = 0 mm, square FOV = 24 cm, TE = 104.4 msec, TI = 1800 msec, TR = 7200 msec, 128×128 image matrix with half-Fourier acquisition. The imaging time for each sequence was 9 min.

The images were displayed and analyzed using in-house-written IDL software. Regions of interest (ROIs) were selected in the white matter (frontal white matter, optic radiations, and centrum semiovale) and gray matter (occipital, parietal, and temporal cerebral cortex) on the first image in the series with weak diffusion weighting. For the five subjects a total of 156 ROIs were selected in the white matter with a mean area of 190 pixels, and 140 ROIs were selected in the cerebral cortex with a mean area of 185 pixels. For each ROI the signal decay was fitted to Eq. [1] using the Marquardt-Levenberg algorithm assuming one or two exponentials (preliminary studies indicated that the best fit was obtained with no more than two exponentials).

The goodness-of-fit was calculated from χ^2 and an index of satisfaction of the fit, IS, derived from the probability distribution P of χ^2 (22).

$$\text{IS}(n/2, \chi^2/2) = 1 - P(n/2, \chi^2/2) = \frac{\Gamma(n/2, \chi^2/2)}{\Gamma(n/2)} \quad [2]$$

where n is the number of degrees of freedom and Γ is the gamma-variate function. A value smaller than 0.001 for IS leads to the rejection of the model, while a value larger than 0.001 is considered to be compatible with the model (22).

To investigate possible transverse relaxation differences in the two components, experiments were repeated on two of the volunteers with $t_D = 24.7 \text{ msec}$, as described above, but with TE varied in steps of 22 msec from 84.4 msec to 170.2 msec. The inversion pulse was not used in these experiments as the analysis of the signal decay data was confined to the deep white matter of the centrum semiovale (with an average area of 200 pixels) remote from CSF. The imaging time was 1 min and 40 sec for each of the five scans.

An investigation of the anisotropy of the individual diffusion components in white matter was then performed. Because useful diffusion anisotropy information can be obtained when white matter fibers are well aligned with the gradient axes (the off-diagonal elements of the diffusion tensor expressed in the gradient reference frame should be negligible), the corpus callosum (the fibers of which run from left to right in an axial slice) was initially selected for study. It was noted from these preliminary studies, however, that a periodic variation of the signal was obtained at b factors $> 2000 \text{ sec mm}^{-2}$, which persisted despite the use of cardiac gating. This precluded an acceptable fit of the signal decay to the biexponential function. Given the close proximity of this structure to the CSF, and the high level of motion sensitivity, this periodicity was attributed to pulsatile brain motion associated with the cardiac cycle. The internal capsule, which also satisfies the orientation criteria, is more remote from CSF

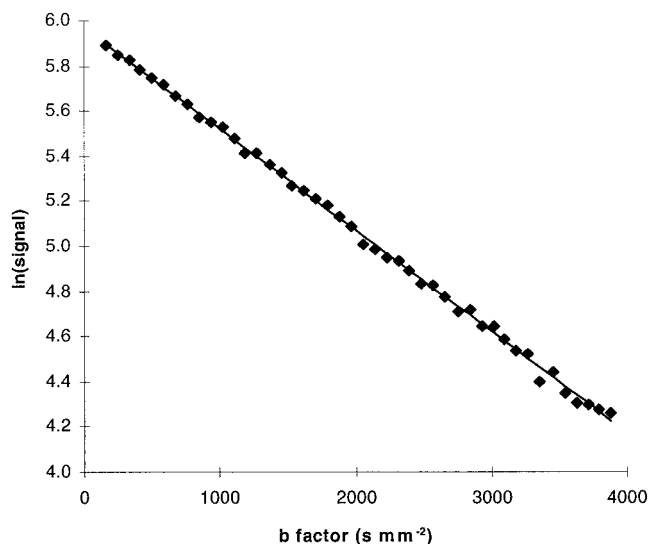


FIG. 1. Diffusion attenuation in isopropanol at 22°C indicating a linear signal decay.

pulsations and provided signal attenuation data that was relatively free of periodic signal variations, resulting in an acceptable biexponential fit.

Echo planar diffusion imaging was then performed on four subjects in the manner described previously, but without the inversion pulse (because the internal capsule is remote from the CSF) and with the addition of gating by means of a pulse oximeter on the subject's finger. Diffusion sensitization was applied along the three orthogonal gradient axes in turn. A single axial slice was selected and the b factor was incremented from 0 to 3800 sec mm⁻² as before, with TE = 104.4 msec and TR equal to twice the RR interval. A trigger delay of 200 msec between the peak of the R wave and the beginning of the sequence was used. The total imaging time was 3 min and 30 sec for the three sampled directions. Analysis of the signal attenuation for each direction of diffusion sensitization was performed as described previously. ROIs were selected on the internal capsule on both the right and left sides of the brain containing an average of 55 pixels. For comparative purposes, a monoexponential fit of the first 11 points, corresponding to b values up to ~1000 sec mm⁻² was performed for each ROI.

RESULTS

The signal decay as a function of b factor for the isopropanol, shown in Fig. 1, was found to be monoexponential as expected. The diffusion coefficient obtained from the fit was $(0.450 \pm 0.004) \times 10^{-3}$ mm² sec⁻¹ in close agreement with a value obtained by Mulkern et al. (17) of 0.44×10^{-3} mm² sec⁻¹.

In the human brain, the fit of the signal decay data assuming a single exponential model was ruled out, as it led to IS < 0.001 in all cases. Indeed, the data were compatible with a biexponential model in all gray and white matter ROIs studied with IS > 0.001. Typical signal decay data from gray and white matter regions are shown in Fig.

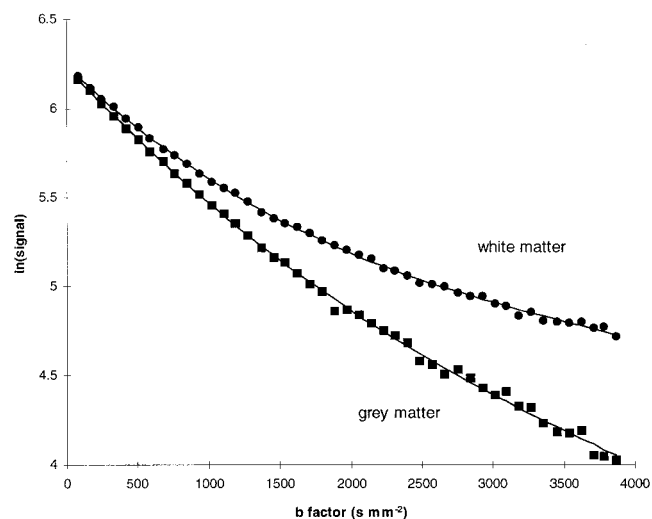


FIG. 2. Typical biexponential decay curves for ROIs in white matter (circles) and gray matter (squares).

2. Table 1 summarizes the values of ADC_{fast}, ADC_{slow}, and f_{fast} averaged over all the gray and white matter ROIs studied for the two diffusion times. Comparison of the grouped white and gray matter fitted parameters obtained for the two diffusion times, corrected for multiple comparisons, indicated that there was no significant difference in any of the fitted parameters between the two examinations. This suggests that ADC_{fast}, ADC_{slow}, and f_{fast} are diffusion time independent between t_D = 24.7 and 57.7 msec.

Comparison of the fitted parameters revealed significant differences ($P < 0.001$) in each parameter for white and gray matter. This difference was apparent for both of the diffusion times studied. In summary, it was found that white matter ADC_{slow} was smaller than gray matter ADC_{slow}, while white matter ADC_{fast} was larger than gray matter ADC_{fast}. The white matter f_{fast} was smaller than the gray matter f_{fast}.

Analysis of the signal decay in the centrum semiovale ROIs revealed that there was no significant difference in the fractional contribution or the fast and slow ADCs as a function of TE. The fractional contribution of the fast diffusion component is plotted against TE for a single representative ROI in Fig. 3. The error bars refer to the standard deviation of the fitted parameter obtained from the Marquardt-Levenberg fit.

Table 1
The Fast and Slow ADC, ADC_{fast} and ADC_{slow} and Fast Diffusing Fraction f_{fast} Averaged Over 156 White Matter and 140 Gray Matter ROIs With t_D = 24.7 ms and t_D = 57.7 ms

t _D	ROI	ADC _{slow}	ADC _{fast}	f _{fast}
24.7 ms	White matter	0.16 ± 0.04	1.12 ± 0.10	0.66 ± 0.10
24.7 ms	Gray matter	0.19 ± 0.07	1.02 ± 0.10	0.70 ± 0.08
57.7 ms	White matter	0.16 ± 0.04	1.13 ± 0.11	0.65 ± 0.06
57.7 ms	Gray matter	0.18 ± 0.07	1.01 ± 0.10	0.73 ± 0.08

The ADC values are reported in units $\times 10^{-3}$ mm² s⁻¹. Error quoted is the standard deviation.

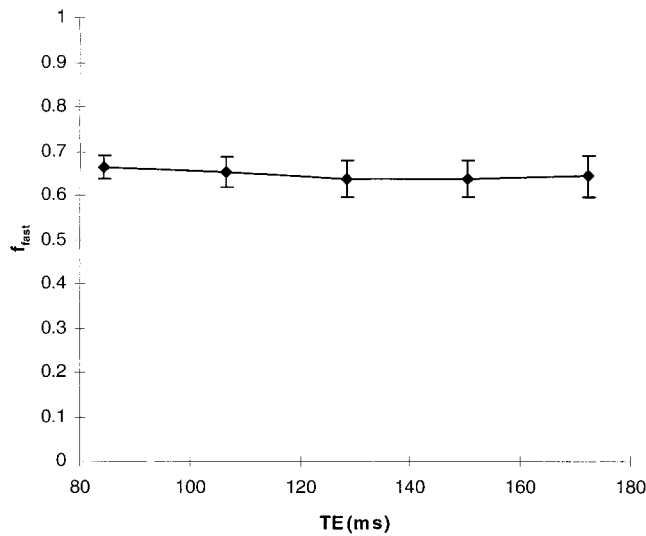


FIG. 3. The fast diffusion volume fraction plotted as a function of echo time.

Biexponential fitting of the signal attenuation data with diffusion sensitization along each of the three gradient axes in turn revealed anisotropy in ADC_{fast} , ADC_{slow} , and f_{fast} . Figure 4 shows an axial slice through the internal capsule (a) in the absence of diffusion-sensitization and with high diffusion-weighting ($>3500 \text{ sec mm}^{-2}$) along the (b) read (right-left), (c) phase (anterior-posterior), and (d) slice (superior-inferior) directions, respectively. Note the strikingly different contrast in the diffusion-weighted images as the direction of sensitization is altered. Typical signal decay data in the internal capsule with diffusion sensitization in the read (right-left), phase (anterior-posterior), and slice (superior-inferior) directions is shown in Fig. 5.

To compare the degree of anisotropy in each parameter, an anisotropy index (AI) proposed by van Gelderen (23) was calculated in each case. Although this index is not

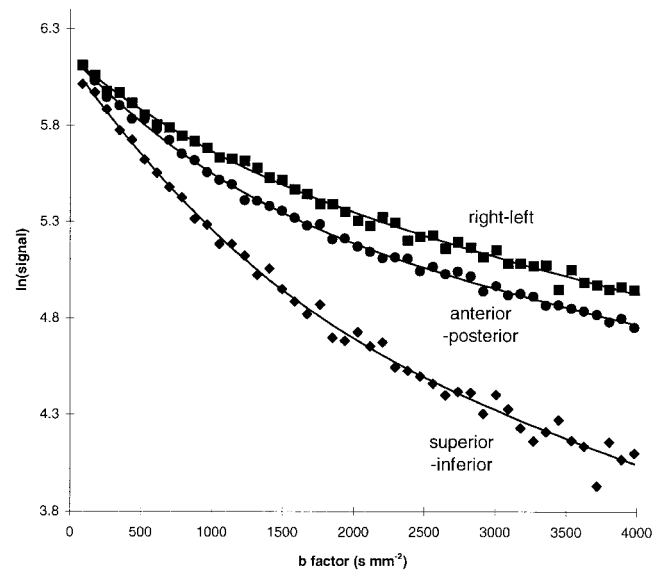


FIG. 5. Biexponential decay curves for a ROI in the internal capsule with diffusion along the read (right-left, squares), phase (anterior-posterior, circles), and slice (superior-inferior, diamonds) directions corresponding to two directions transverse to the fibers and along the direction of the fibers.

truly quantitative, in the sense that it is not rotationally invariant, it provides useful information when the fiber direction is approximately aligned with the gradient axes, as is the case in the internal capsule. A summary of the fitted parameters averaged over the eight ROIs studied is given in Table 2. The AI was found to be highest for ADC_{slow} .

DISCUSSION

This study confirms that when using b factors up to $\sim 4000 \text{ sec mm}^{-2}$ the signal attenuation in human brain is well described by a biexponential decay. The fitted parameters

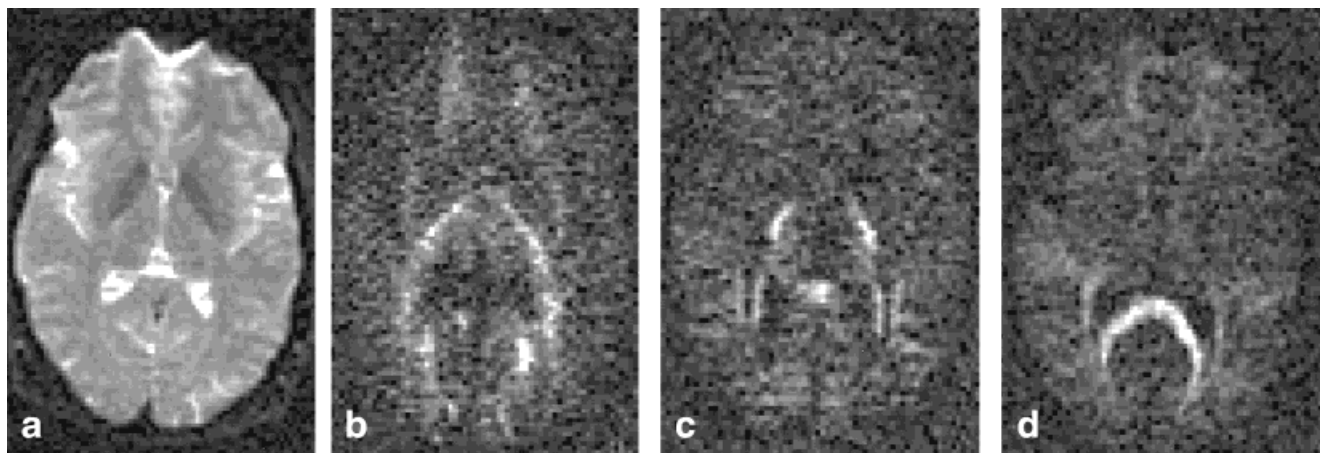


FIG. 4. **a**: A non-diffusion-weighted image and set of diffusion-weighted images using high b factors ($>3500 \text{ sec mm}^{-2}$) with sensitization along **(b)** the read (right-left), **(c)** phase (anterior-posterior), and **(d)** slice (superior-inferior) directions. Note the strikingly different contrast in the white matter structures as the direction of sensitization is altered. The internal capsules are particularly prominent in **d** and appear as two bright regions in each hemisphere near the center of the slice.

Table 2
The Fast and Slow ADC, ADC_{fast} and ADC_{slow} and Fast Diffusing Fraction f_{fast} Obtained With Diffusion Sensitisation Along the Three Orthogonal Gradient Axes

	Read	Phase	Slice	Mean diffusivity	AI
ADC_{slow}	0.14 ± 0.02	0.13 ± 0.02	0.23 ± 0.02	0.17 ± 0.02	0.23 ± 0.10
ADC_{fast}	1.12 ± 0.05	1.13 ± 0.09	1.39 ± 0.11	1.21 ± 0.04	0.08 ± 0.05
f_{fast}	0.50 ± 0.05	0.57 ± 0.03	0.70 ± 0.06	0.59 ± 0.02	0.12 ± 0.06
ADC	0.51 ± 0.04	0.59 ± 0.03	0.89 ± 0.07	0.67 ± 0.02	0.23 ± 0.04

The ADC value is obtained from a linear fit using data acquired with the first 11 points up to $b = 1000 \text{ s mm}^{-2}$ only. The AI represents the anisotropy index calculated from the squared deviations of the ADC along three orthogonal directions as described by van Gelderen et al. (23). The ADC values are reported in units $\times 10^{-3} \text{ mm}^2 \text{ s}^{-1}$. Error quoted is the standard deviation.

ADC_{fast} , ADC_{slow} , and f_{fast} obtained in the gray and white matter are similar to those obtained by Mulkern et al. (17) using b factors up to 6000 sec mm^{-2} . Mulkern et al. (17) obtained $ADC_{fast} = (1.40 \pm 0.26) \times 10^{-3} \text{ mm}^2 \text{ sec}^{-1}$ and $ADC_{slow} = (0.25 \pm 0.03) \times 10^{-3} \text{ mm}^2 \text{ sec}^{-1}$ with $f_{fast} = 0.74 \pm 0.02$. Grouping the white and gray matter data together we obtain $ADC_{fast} = (1.07 \pm 0.17) \times 10^{-3} \text{ mm}^2 \text{ sec}^{-1}$ and $ADC_{slow} = (0.17 \pm 0.06) \times 10^{-3} \text{ mm}^2 \text{ sec}^{-1}$ with $f_{fast} = 0.69 \pm 0.02$. One notable difference between the two studies, however, is the long TE of 175 msec employed by Mulkern et al. to accommodate sufficiently long gradient pulses to achieve the diffusion sensitivity necessary with their line-scan approach, which resulted in a lower signal-to-noise ratio (SNR) than was obtained here. Differences in the fitted parameters between the two studies may be partly due to differences in the proportions of white and gray matter studied, in addition to the different b factor ranges which may also influence the results, although this latter point has yet to be investigated.

Assignment of the Fast and Slow Diffusion Compartments to the Intra- and Extracellular Spaces in Human Brain

The observation of biexponential diffusion decay is suggestive of two water diffusion compartments in human brain. Although non-monoexponential diffusion decay may arise from restricted diffusion (24), this would not necessarily give rise to a biexponential diffusion decay. Background gradients generated within the tissue structure may also give a non-monoexponential decay (25); however, a recent study by Clark et al. (26) indicated that susceptibility-induced background gradient influences on the estimated ADC are insignificant at 1.5 T. Partial volume of CSF in the ROIs, which may also give rise to non-monoexponential decay, was eliminated by the use of an inversion pulse prior to the diffusion-weighted sequence.

The assignment of the slow and fast diffusing fraction to the intra- and extracellular spaces is not straightforward, given the discrepancy between the f_{fast} estimate obtained from study of biexponential diffusion attenuation and the expected intra- and extracellular volume fractions (15,17), assuming that the extracellular water is represented by the fast diffusing fraction. The possibility that the intra- and extracellular compartments have different T_2 values has been raised previously to explain this discrepancy (15). If this hypothesis is true, one might expect to obtain a TE dependence in the fitted component fractions. In the

present study it was observed that the fitted fractions were independent of the TE chosen, in agreement with the findings of Niendorf et al. (15) for the rat brain. It would appear, therefore, that the T_2 values of the two compartments are similar and do not explain the discrepancy between the known volume fractions for the intra- and extracellular space and those estimated by high b value diffusion measurements.

A number of other factors which may affect the estimate of the volume fractions include the possibility of appreciable exchange between the compartments during the diffusion time and differences in the T_1 and proton density of the two pools. Li et al. (27) pointed out that if the exchange is significant (but not fast), the contribution of the slow diffusion component is underestimated. Thus, appreciable exchange between compartments may explain the underestimation of the slow diffusion volume fraction in this and other studies. The issue of possible T_1 differences in the compartments was addressed in a recent study by Mulkern et al. (28) using inversion pulses with a range of inversion times of 40–500 msec. It was found that there was no statistically significant difference in the T_1 values of the slow and fast diffusion fractions in both the cortical gray matter and internal capsule in the human brain. Proton density differences in the two pools may also lead to discrepancies in the estimated volume fractions, as may the lack of contribution from NMR invisible water.

The assignment of the slow and fast diffusion fractions to the intra- and extracellular spaces may be further complicated by the resolution of more than two components when very high b factors (higher than employed here) are used. This has been found in rat brain in vivo using b factors up to $300,000 \text{ sec mm}^{-2}$ (29). The resolution of further water diffusion components may correspond, for example, to intracellular substructures and organelles, and presumably are not observed in our experiments. Further investigation of these very slowly diffusing components in the human brain in vivo is restricted somewhat by the gradient amplitude limitations of whole body MRI systems. However, the lack of contribution from these components in our experiments may also be compatible with the overestimation of the fast diffusion component fraction.

Although the discrepancy between the intra- and extracellular volume fractions and the slow and fast diffusion fractions has yet to be resolved, it is worth noting the similarity between ADC_{fast} and the ADC for the extracel-

lular space predicted from tortuosity models and experiments based on the diffusion of tetramethylammonium ions (TMA) (16). For example, using the tortuosity factor for white matter in rat brain ($\lambda = 1.55$) obtained by Lehmenkuhler et al. (30), and the free diffusion value of water at 37°C extracted from Harris et al. (31) by linear regression ($D = 3.05 \times 10^{-3} \text{ mm}^2 \text{ sec}^{-1}$), the predicted extracellular diffusion coefficient according to Eq. [3]

$$\text{ADC}_{\text{extra}} = \frac{D}{\lambda^2} \quad [3]$$

is $1.27 \times 10^{-3} \text{ mm}^2 \text{ sec}^{-1}$. This is of the same order of magnitude as the fast diffusion fraction found in human brain white matter, $\text{ADC}_{\text{fast}} = 1.12 \times 10^{-3} \text{ mm}^2 \text{ sec}^{-1}$. It is also noteworthy that the lower gray matter ADC_{fast} compared with white matter ADC_{fast} is compatible with predictions based on TMA diffusion in the rat cortex where the tortuosity factor is generally larger in the gray matter than for the white matter ($\lambda = 1.65$ at level IV of the cortex). In summary, our findings provide suggestive evidence for the assignment of the fast diffusion component to the extracellular space.

The reasons for the difference in the fitted parameters between white and gray matter remain unknown. However, it is possible that the myelin, in which water may be expected to diffuse more slowly, may result in a lower ADC_{slow} and a smaller weighting of the fast diffusing fraction in white matter.

Diffusion Time Dependence of the Two Diffusion Compartments

Comparison of the signal decay data at the two diffusion times studied indicates that the fitted parameters are diffusion time independent between $t_D = 24.7$ and 57.7 msec. This finding would appear to be compatible with that of Le Bihan et al. (32), which demonstrated the absence of any diffusion time dependence in the ADC obtained from a monoexponential fit of decay data obtained in human brain white matter with t_D between 16 and 79 msec. If the fast diffusing component does originate from the extracellular space, it is worth noting that it is this component which predominates in ADC estimations using monoexponential decay analysis and b factors up to $\sim 1500 \text{ sec mm}^{-2}$. This result is not surprising if water diffusion is simply hindered by white matter fibers, as there is no actual physical limit to the diffusion path (9). The lack of diffusion time dependence observed in this study for the slow diffusing component may be due to a steady-state effect whereby all the MRI visible intracellular molecules have interacted with the permeable cell walls. Theoretical studies of diffusion time dependence in spinal cord tissue indicate that very short diffusion times (33) on the order of microseconds may be required to observe significant increases in the ADC, as fewer diffusing molecules interact with the surrounding structure. Furthermore, the fact that ADC_{slow} is approximately six times smaller than ADC_{fast} is suggestive of impeded (restricted and/or hindered) diffusion in this compartment. These results also indicate that an important change in the rate of exchange between the two compartments at the diffusion times studied is un-

likely. The identification and separation of the diffusion time dependence of the fast and slow compartments is clearly an attractive means with which to further our understanding of tissue water diffusion dynamics, but given the hardware limitations on whole body MRI systems, it is more likely to be realized in animal studies than in those performed in the human brain.

Anisotropy in the Slow and Fast Water Diffusion Compartments

Biexponential fitting of the signal decay with diffusion sensitization along each of the three orthogonal gradient directions, approximately corresponding to the longitudinal and two perpendicular transverse axes of the internal capsule, indicated anisotropy in both ADC_{fast} and ADC_{slow} (see Table 2). The observation of anisotropy in both these compartments is compatible with the morphological similarity in the intra- and extracellular spaces, given that the latter is formed around the former. Based on the calculation of the van Gelderen index (23) for each of these compartments it would appear that ADC_{slow} is more anisotropic than ADC_{fast} . Although this observation is consistent with a restricted intracellular space and tortuous extracellular space, it should be noted that the lower precision in the estimate of ADC_{slow} may tend to overestimate the apparent anisotropy, as discussed previously by Pierpaoli et al. (34) for noisy monoexponential data. Overestimation in the anisotropy of ADC_{fast} would occur to a lesser extent due to the higher precision in this parameter. In the context of new fiber-tracking methodology, it is worth remarking that it is likely to be the extracellular spaces surrounding the white matter fiber bundles that are being tracked since b factors $\sim 1000 \text{ sec mm}^{-2}$ are used for determining the apparent diffusion tensor. The enhanced diffusion anisotropy in the slow diffusion fraction may, however, provide a new and more powerful contrast for fiber tracking methodologies.

Surprisingly, the fraction of spins attributed to each of the components also changed with the direction of diffusion sensitization, appearing anisotropic with f_{fast} higher along the tracts than across them. This phenomenon has also recently been observed by Assaf and Cohen (35) in the excised optic nerve of the rat. This observation may result from the assumption of the "no exchange criterion" embedded in Eq. [1]. Given that changing the exchange rates in the Karger equations (17,36) (which allow for exchange between the two compartments) also changes the value of f_{fast} , we may hypothesize that the apparent anisotropy in f_{fast} is caused by a directional dependence in the exchange rates. For example, one may envisage that the probability of exchange along the axon may be significant, whereas this probability may be lower across the axon cylinder. In this case there may be a continuum of exchange rates in white matter owing to the variable orientation of fiber tracts in the brain. This model would explain the higher value of f_{fast} along the direction of the internal capsule compared with the perpendicular, transverse directions. Clearly, this hypothesis requires further investigation and may be examined more closely by performing experiments at short diffusion times that satisfy the no-exchange conditions in all directions, which may remove anisotropy in

the estimate of f_{fast} . Unfortunately, a reduction in the diffusion time generally results in a reduction in the overall diffusion sensitivity for a given maximum gradient strength, and it is probable that sufficiently short diffusion times at sufficiently large b values may only be achievable on MRI systems designed for animal studies.

It is worth remarking that anisotropy in white matter ADC_{fast} is predicted from tortuosity models of TMA diffusion in the extracellular space. Within the corpus callosum of the rat brain, Mazel et al. (37) obtained $\lambda = 1.47$ along the fibers, and $\lambda = 1.67$ and 1.69 perpendicular to the fibers. Using Eq. [3] and the free diffusion value of water at 37°C from Harris et al. (31), one obtains $\text{ADC}_{\text{fast}} = 1.41 \times 10^{-3} \text{ mm}^2 \text{ sec}^{-1}$ along the fibers, $\text{ADC}_{\text{fast}} = 1.09 \times 10^{-3} \text{ mm}^2 \text{ sec}^{-1}$ and $1.07 \times 10^{-3} \text{ mm}^2 \text{ sec}^{-1}$ perpendicular to the fibers, and $\text{AI} = 0.1$. These values are similar to the values of ADC_{fast} and AI obtained from study of biexponential diffusion decay in the human internal capsule (see Table 2).

Implications for the ADC Determined With Single Exponential Fitting Using b Factors Smaller Than 1500 sec mm^{-2}

One should consider that the fast diffusing fraction predominates the MRI signal at low b values (less than 1500 sec mm^{-2}), as used in most clinical studies and animal experiments, especially when data are fitted to a single exponential.

This has important implications for the assessment of diffusion behavior in tissues, as during ischemia or white matter anisotropy. For instance, these findings suggest that the observed diffusion anisotropy in white matter is likely to be determined by the anisotropic tortuosity of the extracellular space between aligned fibers rather than to restricted diffusion inside the myelinated axons. Thus, tracking strategies based on the directional characteristics of the diffusion tensor probably depend on the diffusional properties of water in the extracellular space rather than in the axons themselves. The application of diffusion tensor methodology in the separation of slow and fast diffusing components in the human brain is clearly appealing. In particular, the possibility of identifying the diffusional properties of the intracellular space may have important implications for neuronal fiber tracking methodology. This would allow the intra-axonal space rather than the extracellular space to be tracked, which in turn may have other important applications—such as the resolution of crossing or diverging fibers. This may prove to be difficult however, due to the high SNR and large number of diffusion-weighted images that would be required for a reliable fit of the data on a pixel by pixel basis. Furthermore, our investigations of diffusion signal decay at high b factors in the corpus callosum suggest that brain pulsation and motion may also be a confounding factor.

Due to the non-monoexponential nature of the diffusion signal decay, the choice of b factors when using a monoexponential fit will influence the value of the ADC measured. If higher b factors are used, more of the slow diffusion fraction will be sampled, reducing the value of the overall estimated ADC. As an example, consider the ADC determined from only two b values as shown in Fig. 6,

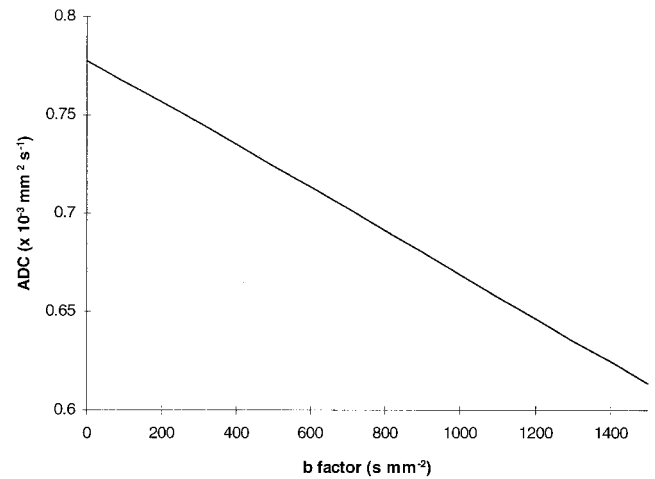


FIG. 6. Plot of the estimated ADC using only two b factors. The value of the estimated ADC declines as the maximum b factor increases.

which depicts the value of the ADC as a function of maximum b factor (with a minimum b factor set to zero) based on the white matter biexponential decay data with $t_D = 24.7$ msec. Over the range of maximum b factors from 500 to 1500 sec mm^{-2} (typically used in most diffusion studies), the estimated ADC decreases from $0.72 \times 10^{-3} \text{ sec mm}^{-2}$ by 15% to $0.61 \times 10^{-3} \text{ sec mm}^{-2}$. Thus careful attention should be paid to the b factors used when comparing studies across sites, particularly those aimed at examining subtle changes in brain water diffusion due to diffuse pathology. In acute brain ischemia, the observed ADC decrease may largely originate from a simple volume effect (shrinkage of the extracellular space), taking into account the predominant contribution of the fast component to the diffusion-sensitized MR signal.

CONCLUSION

We have used a simple biexponential analysis to describe the diffusion signal decay in human brain when b factors up to $\sim 4000 \text{ sec mm}^{-2}$ are used. This analysis confirmed that water diffusion in the human brain can be resolved into a fast and a slow diffusing fraction, both in gray and white matter. Reconciliation of the observed compartments with the intra- and extracellular water is complicated by the discrepancy between the known volume fractions and those estimated using water diffusion measurements if the fast diffusing fraction is attributed to the extracellular space. A possible bias in the estimated volume fractions due to differences in the T_2 values of the two compartments is ruled out by the lack of a relationship between the estimated volume fractions and TE, in agreement with a previous rat brain study. The failure to resolve distinct T_2 values in the compartments is consistent with a process of significant exchange between the compartments during the diffusion time, resulting in an underestimation of the slow diffusion volume fraction. However, the magnitude of ADC_{fast} , degree of anisotropy in ADC_{fast} in white matter, and differences between white and gray matter determined from biexponential signal decay analy-

sis are in agreement with predictions of the extracellular ADC of water based on tortuosity models and measurement of TMA diffusion in rat brain. This provides suggestive evidence for the assignment of the fast diffusion fraction to the extracellular space.

Directional study of the diffusion signal decay in white matter revealed diffusion anisotropy in both the fast and slowly diffusing water spaces. Interestingly, anisotropy was also found in the fraction of spins attributed to each of the compartments. This anisotropy may result from a difference in the exchange rate between the fast and slow diffusion compartments depending on the orientation of the white matter fibers with respect to the measurement direction. The main difficulty in validating this hypothesis, however, is that the exchange rates between the two compartments are largely unknown, especially in the human brain. Further experiments performed at diffusion times which are sufficiently short to impose the no-exchange condition should help to validate this hypothesis, and may provide new information concerning the nature of the water compartments resolved using high b factors.

ACKNOWLEDGMENTS

C.A.C. is partly supported by EEC BioMed grant #BMH4-CT96-0870. The authors thank Hugues Chabriat for his assistance with the statistical analysis.

REFERENCES

- Pierpaoli C, Jezzard P, Basser PJ, Barnett A, Di Chiro G. Diffusion tensor MR imaging of the human brain. *Radiology* 1996;201:637–648.
- Lutsep HL, Albers GW, de Crespigny A, Kamat GN, Marks MP, Moseley ME. Clinical utility of diffusion-weighted magnetic resonance imaging in the assessment of ischemic stroke. *Ann Neurol* 1997;41:574–580.
- Werring DJ, Clark CA, Barker GJ, Thompson AJ, Miller DH. Diffusion tensor imaging of lesions and normal appearing white matter in multiple sclerosis. *Neurology* 1999;52:1626–1632.
- Sugahara T, Korogi Y, Kochi M, Ikushima I, Shigematu Y, Hirai T, Okuda T, Liang L, Ge Y, Komohara Y, Ushio Y, Takahashi M. Usefulness of diffusion-weighted MRI with echo-planar technique in the evaluation of cellularity in gliomas. *J Magn Reson Imaging* 1999;9:53–60.
- Wiesmann UC, Clark CA, Symms MR, Barker GJ, Birnie KD, Shorvon S.D. Water diffusion in the human hippocampus in epilepsy. *Magn Reson Imaging* 1999;17:29–36.
- Bahn MM, Kido DK, Lin W, Pearlman AL. Brain magnetic resonance diffusion abnormalities in Creutzfeldt-Jakob disease. *Arch Neurol* 1997;54:1411–1415.
- Lim KO, Hedehus M, Moseley M, de Crespigny A, Sullivan EV, Pfefferbaum A. Compromised white matter tract integrity in schizophrenia inferred from diffusion tensor imaging. *Arch Gen Psychiatry* 1999;56:367–374.
- Werring DJ, Clark CA, Barker GJ, Miller DH, Parker GJM, Brammer MJ, Bullmore ET, Giampietro VP, Thompson AJ. The structural and functional mechanisms of motor recovery: complementary use of diffusion tensor and functional magnetic resonance imaging in a traumatic injury of the internal capsule. *J Neurol Neurosurg Psych* 1998;65:863–869.
- Le Bihan D. Molecular diffusion, tissue microdynamics and microstructure. *NMR Biomed* 1995;8:375–386.
- Moseley ME, Cohen Y, Kucharczyk J, Mintorovitch J, Asgari HS, Wendland MF, Tsuruda J, Norman D. Diffusion-weighted MR imaging of anisotropic water diffusion in the cat central nervous system. *Radiology* 1990;176:439–445.
- Douek P, Turner R, Pekar J, Patronas N, Le Bihan D. MR color mapping of myelin fiber orientation. *J Comp Assist Tomogr* 1991;15:923–929.
- Basser PJ, Mattiello J, Le Bihan D. MR diffusion tensor spectroscopy and imaging. *Biophys J* 1994;66:259–267.
- Cooper RL, Chang DB, Young AC, Martin CJ, Ancker-Johnson B. Restricted diffusion in biophysical systems. *Biophys J* 1974;14:161–177.
- Latour LL, Svoboda K, Mitra PP, Sotak CH. Time-dependent diffusion of water in a biological model system. *Proc Natl Acad Sci USA* 1994;91:1229–1233.
- Niendorf T, Dijkhuizen RM, Norris DG, van Lookeren Campagne M, Nicolay K. Biexponential diffusion attenuation in various states of brain tissue: implications for diffusion-weighted imaging. *Magn Reson Med* 1996;36:847–857.
- Nicholson C, Sykova E. Extracellular space structure revealed by diffusion analysis. *Trends Neurosci* 1998;21:207–215.
- Mulkern RV, Gudbjartsson H, Westin C-F, Zengingonul HP, Gartner W, Guttman CRG, Robertson RL, Kyriakos W, Schwartz R, Holtzman D, Jolesz FA, Maier SE. Multi-component apparent diffusion coefficients in human brain. *NMR Biomed* 1999;12:51–62.
- Mori S, Crain BJ, Chacko VP, van Zijl PCM. Three-dimensional tracking of axonal projections in the brain by magnetic resonance imaging. *Ann Neurol* 1999;45:265–269.
- Jones DK, Simmons A, Williams SCR, Horsfield MA. Non-invasive assessment of axonal fiber connectivity in the human brain via diffusion tensor MRI. *Magn Reson Med* 1999;42:37–41.
- Poupon C, Clark CA, Frouin V, Bloch I, Le Bihan D, Mangin JF. Tracking white matter fascicles with diffusion tensor imaging. In: Proceedings of the 7th Annual Meeting of ISMRM, Philadelphia, 1999. p 325.
- Conturo TE, Lori NF, Cull TS, Akbudak E, Snyder AZ, Shimony JS, McKinstry RC, Burton H, Raichle ME. Tracking neuronal fiber pathways in the living human brain. *Proc Natl Acad Sci USA* 1999;96:10422–10427.
- Press WH, Teulosky SA, Vetterling WT, Flannery BP. Numerical recipes in C. Cambridge: Cambridge University Press; 1992.
- van Gelderen P, de Vleeschouwer MHM, DesPres D, Pekar J, van Zijl PCM, Moonen CTW. Water diffusion and acute stroke. *Magn Reson Med* 1994;31:154–163.
- Hurlimann MD, Helmer KG, De Swiet TM, Sen PN, Sotak CH. Spin echoes in a constant gradient and in the presence of simple restriction. *J Magn Reson Series A* 1995;113:260–264.
- Zhong J, Gore JC. Studies of restricted diffusion in heterogeneous media containing variations in susceptibility. *Magn Reson Med* 1991;19:276–284.
- Clark CA, Barker GJ, Tofts PS. An in vivo evaluation of the effects of local susceptibility gradients on water diffusion measurements in human brain. *J Magn Reson* 1999;141:52–61.
- Li JC, Stanisz GJ, Henkelman RM. Integrated analysis of diffusion and relaxation of water in blood. *Magn Reson Med* 1998;40:79–88.
- Mulkern RV, Zengingoul HP, Holtzman D, Guttman CRG, Robertson RL, Kyriakos W, Jolesz FA, Maier SE. Multi-component apparent diffusion coefficients in human brain: grey/white matter differences and spin lattice relaxation times. In: Proceedings of the 7th Annual Meeting of ISMRM, Philadelphia, 1999. p 1806.
- Pfeuffer J, Provencher SW, Gruetter R. Water diffusion in rat brain in vivo as detected at very large b values is multicompartmental. *MAGMA* 1999;8:98–108.
- Lehmenkuler A, Sykova E, Svoboda J, Zilles K, Nicholson C. Extracellular space parameters in the rat neocortex and subcortical white matter during postnatal development determined by diffusion analysis. *Neuroscience* 1993;55:339–351.
- Harris KR, Woolf LA. Pressure and temperature dependence of the self diffusion coefficient of water and oxygen-18 water. *J Chem Soc-Faraday Trans I* 1980;76:377–385.
- Le Bihan D, Turner R, Douek P. Is water diffusion restricted in human brain white matter? An echo planar NMR imaging study. *NeuroReport* 1993;4:887–890.
- Ford JC, Hackney DB, Lavi E, Phillips M, Patel U. Dependence of apparent diffusion coefficients on axonal spacing, membrane permeability and diffusion time in spinal cord white matter. *J Magn Reson Imaging* 1998;8:775–782.
- Pierpaoli C, Basser PJ. Toward a quantitative assessment of diffusion anisotropy. *Magn Reson Med* 1996;36:893–906.
- Assaf Y, Cohen Y. Assignment of the water slow-diffusing component in the central nervous system using q-space diffusion MRS: implications for fiber tract imaging. *Magn Reson Med* 2000;43:191–199.
- Karger J, Pfeifer H, Heink W. Principles and applications of self-diffusion measurements by NMR. *Adv Magn Reson* 1988;12:1–89.
- Mazel T, Simonova Z, Sykova E. Diffusion heterogeneity and anisotropy in rat hippocampus. *Neuroreport* 1998;9:1299–1304.